U. of Iowa 70:35

Distribution of this document is unlimited.

N 70 36984

CR 112770

POYNTING FLUX STUDIES OF HISS WITH THE INJUN 5 SATELLITE*

Stephen R. Mosier**

*This work was supported in part by the Office of Naval Research under Contract No. N00014-68-A-0196-0003

Department of Physics and Astronomy
THE UNIVERSITY OF IOWA
Iowa City, Iowa

U. of Iowa 70-35

POYNTING FLUX STUDIES OF HISS WITH THE INJUN 5 SATELLITE*

Stephen R. Mosier**

Department of Physics and Astronomy
The University of Iowa
Iowa City, Iowa 52240

April 1970

*This research was supported in part by the National Aeronautics and Space Administration under Contracts NAS5-10625, NAS1-8141, NAS1-8144(f), NAS1-8150(f), and NGR-16-001-043; and by the Office of Naval Research under Contract N00014-68-A-0196-003.

**Present address: NASA/Goddard Space Flight Center
Greenbelt, Maryland 20771

UNCLASSIFIED

Security Classification

DOCUMENT CONTROL DATA - R&D

(Security classification of title, body of abstract and indexing annotation must be entered when the overall report is classified)

1. ORIGINATING ACTIVITY (Corporate author) University of Iowa Department of Physics and Astronomy	2a. REPORT SECURITY CLASSIFICATION UNCLASSIFIED 2b. GROUP

3. REPORT TITLE

Poynting Flux Studies of Hiss with the Injun 5 Satellite

4. DESCRIPTIVE NOTES (Type of report and inclusive dates)

Progress April 1970

5. AUTHOR(S) (Last name, first name, initial)

Mosier, Stephen R.

6. REPORT DATE April 1970	7a. TOTAL NO. OF PAGES 37	7b. NO. OF REFS 13

8a. CONTRACT OR GRANT NO. N00014-68-A-0196-003 b. PROJECT NO. c. d.	9a. ORIGINATOR'S REPORT NUMBER(S) Research Report 70-35 9b. OTHER REPORT NO(S) (Any other numbers that may be assigned this report)

10. AVAILABILITY/LIMITATION NOTICES

Distribution of this document is unlimited.

11. SUPPLEMENTARY NOTES	12. SPONSORING MILITARY ACTIVITY Office of Naval Research

13. ABSTRACT

[SEE FOLLOWING PAGE]

DD FORM 1 JAN 64 1473

UNCLASSIFIED

Security Classification

ABSTRACT

A study of very-low-frequency hiss emissions in the region 677 to 2528 km and 35° to 75° invariant latitude (in the northern hemisphere) using the Injun 5 Poynting flux measurement technique is presented. Downgoing ELF hiss is observed over the entire region of altitude-invariant latitude space under study, whereas ELF hiss having an upward-directed net Poynting flux is only observed at invariant latitudes below about 60°. A new propagation phenomenon is proposed in which downgoing ELF hiss may propagate across the plasmapause boundary to lower latitudes and become subsequently reflected and trapped within the plasmasphere. Measurements indicate that at least part of the VLF hiss which is observed by the Injun 5 satellite must be generated above the Injun 5 altitude range. A new type of sub-auroral-zone VLF hiss has been observed called mid-latitude hiss.

I. INTRODUCTION

This paper reports on studies of very-low-frequency hiss using the Poynting flux measurement techniques of the Injun 5 satellite. The theoretical basis for the Poynting flux measurements with the Injun 5 satellite is presented in the preceding paper [Mosier and Gurnett, 1970], hereafter referred to as Paper 1. The purpose of this paper is to present the results of detailed studies of hiss phenomena beyond those reported by Mosier and Gurnett [1969].

Injun 5 is a low-altitude (677 to 2528 km), polar-orbiting satellite launched on 8 August 1968 and carrying a VLF (30 Hz to 10 kHz) electric and magnetic fields experiment [Gurnett et al., 1969]. The satellite is magnetically oriented such that, when properly aligned, the x axis of the satellite is parallel to the geomagnetic field and the electric antenna axis (y axis) and magnetic antenna axis (z axis) are perpendicular to the geomagnetic field, as well as to each other (see Figure 1). Referring to Paper 1 and making a permutation of coordinate axes for the Injun 5 satellite geometry, it has been shown that, for a single plane wave, the measurement of the time-averaged correlation $\langle E_y B_z \rangle$ between the electric and magnetic signals is sufficient to determine the direction of the Poynting flux $\langle S_x \rangle$ along the geomagnetic field (x axis). For multiple waves such as hiss, certain restrictions must be applied to this correlation measurement. As discussed in Paper 1, the proportionality factor between $<E_y B_z>$ and $<S_x>$ is a function of both the wave normal angle θ and the azimuthal angular orientation of the satellite (refer to the azimuthal coordinate ψ in Paper 1). At frequencies above the local LHR frequency, the proportionality factor goes to zero at the resonance cone for two azimuthal angular positions ($\psi = \pi/2$ and $\psi = 3\pi/2$, as defined in Paper 1). At all other azimuthal satellite orientations, the proportionality factor is nearly isotropic as a function of θ. Below the local LHR frequency, the anisotropy is not so pronounced (the proportionality factor does not go to zero) and as the proton gyrofrequency is approached, the proportionality factor ceases to be a function of the wave normal angle. If a measurement is performed under conditions such that the proportionality factor is highly anisotropic, then one cannot make a definite conclusion regarding the direction of the <u>net</u> Poynting flux of the waves. One can only say that if a correlation for a given direction is observed, then there must be at least <u>some</u> waves propagating in that direction, up or down the field lines. However, if a sufficient number of measurements are made such that they are distributed over the range of azimuthal orientations, then the occurrence of measurements having isotropic proportionality factors (as a function of θ) allows one to accurately determine the <u>net</u> Poynting flux direction. One further qualification must be made: if waves are observed to be propagating both up and down the geomagnetic field, then nothing can be said concerning the relative intensities of the upgoing and downgoing components unless the measurement is performed near the proton gyrofrequency where the proportionality factor is isotropic for all azimuthal orientations. For a description of the correlation measurement technique, the reader is referred to Mosier and Gurnett [1969].

The Injun 5 data presented in this paper were acquired by the North Liberty Data Acquisition FAcility of The University of Iowa during the periods 31 December 1968 through 25 February 1969 and 4 March 1969 through 12 May 1969. Of the 1529 Injun 5 revolutions during these periods, VLF data were acquired for 628 revolutions and data for the Poynting flux measurements were obtained from the study of 329 revolutions. These 329 revolutions were chosen to give a good sampling of both magnetic local day (0600 - 1800 MLT) and magnetic local night (1800 - 0600 MLT) and are distributed throughout the December through May time period. These data cover the range of invariant latitudes (INVL) from approximately 35° to 75°.

II. ELF HISS

A. Results of Observations

In the initial results of the Injun 5 Poynting flux measurements reported by Mosier and Gurnett [1969], 12 examples of ELF hiss had been observed below 1500 km by the Poynting flux measurement technique, the net Poynting flux of which were determined to be directed downward. In addition, reflections of downgoing waves near the two-ion cutoff frequency were observed (see Figure 5 of Mosier and Gurnett [1969]). However, in the more detailed study reported in this paper, ELF hiss has been observed in which the net Poynting flux is directed up the geomagnetic field (in the northern hemisphere). In this section, the results of the ELF hiss study will be discussed and a propagation mechanism will be proposed to explain the observations of upgoing hiss.

Of the 329 Injun 5 revolutions which were studied, ELF hiss was identified in 140 revolutions. The results of the correlation measurements from these 140 revolutions are presented in Figures 2 and 3. In Figure 2, the Injun 5 orbit is plotted, in altitude versus invariant latitude, for all times at which the Poynting flux was observed to be directed down the geomagnetic field. Figure 3 is a similar plot for observations in which the Poynting flux was directed up the field. As can be seen from these plots, downgoing ELF hiss was observed over the entire region of altitude-invariant latitude space under study, whereas the highest latitude at which the net Poynting flux of ELF hiss was directed upward is approximately 60° INVL. Furthermore, with the exception of three isolated observations of less than one minute duration, all observed cases of upgoing ELF hiss below 1500 km occurred at local night, between 1800 and 0600 MLT. It should be noted that the data presented in Figures 2 and 3 overlap in many cases, since both upgoing <u>and</u> downgoing hiss are often observed in the same region.

Since the high-latitude cutoff for upgoing ELF hiss coincides with the approximate location of the plasmapause - light ion trough boundary [Carpenter, 1966; Taylor et al., 1969], data from the AFCRL electron density probe on Injun 5 were examined to find out if the transition in net Poynting flux direction corresponds with the location of the plasmapause boundary for individual cases. In five of 16 cases studied, the transition occurred at lower latitudes, within several degrees of the abrupt decrease in the electron density gradient profile. In the remaining 11 cases, the transition occurred at the same latitude as the abrupt density decrease (R. Sagalyn, personal communication). This abrupt decrease in the electron density gradient may be identified with the plasmapause boundary, although at low altitudes the plasmapause does not always exhibit a well-defined density decrease (D.L. Carpenter, personal communication).

A typical example of the transition in net Poynting flux direction in the region of the plasmapause boundary is illustrated in Figure 4. After a slight peak in electron density at 1414:30 UT, N_e begins to decrease with the largest density gradient, identified as the plasmapause, occurring between 1417:30 and 1418 UT, at approximately 56.5° INVL (L = 3.3). The transition from an upward to a downward-directed net Poynting flux occurs near the plasmapause boundary at about 1418:30 at all frequencies at which the emission is observed. The correlation measurement at 250Hz in Figure 4 intercepts the lower frequency cutoff of the ELF hiss (visible in the 30-650 Hz electric and magnetic spectra) at 1413:30 UT. In this measurement, the net Poynting flux at the cutoff is directed upwards.

Two other features are often present in the 300 Hz to 10 kHz electric receiver spectra at plasmapause crossings and can be seen in Figure 4. First, a breakup in the LHR noise band begins at 1417:40 UT, with the noise continuing until approximately 1420 UT. The LHR breakup at the plasmapause has been identified and discussed by Carpenter et al., [1968]. Secondly, the electric antenna impedance increases sharply between 1418:30 and 1419 UT. Since the impedance is a function of both the electron density and the electron temperature, it must be concluded that either the density or temperature, or both, undergo a rather discontinuous change at that time. The plot of N_e versus time in Figure 4 from the AFCRL probe does not reflect this feature since the electron density calibration is a function of electron temperature and spacecraft potential, neither of which were available at the time these preliminary electron density data were prepared. For the plot in Figure 4, a constant temperature and potential were assumed. Nevertheless, this simplification can only affect the magnitude of the density gradient, but not its general location or features.

As a check on the validity of the transition in the direction of the net Poynting flux, large phase shifts (up to 80°) were introduced in both the electric and magnetic signals prior to making the correlation measurement for a large number of cases in which a transition occurred. Since this transition often occurs at very nearly the same time that a large change in the electric antenna impedance is observed (see Figure 4), and since a large input impedance to the electric preamplifier may produce relative phase shifts between the electric and magnetic signals of the order of 10 to 20°, it might be argued that the observed change in the net

Poynting flux direction is an instrumental effect. However, in all of the cases checked, very large phase shifts (50-80°) were required to change the sign of the correlation measurement for both downgoing and upgoing hiss, indicating that phase errors of the order of 50° or less are not occurring at the receiver input. In addition, in a large number of observations of ELF hiss, short-fractional-hop whistlers were observed simultaneously and were always found to be upgoing, as expected. Whenever short-fractional-hop whistlers were simultaneously observed on both sides of a transition in Poynting flux direction, identical phase shifts were required to change the signs of both the ELF hiss correlation and the whistler correlation measurements, giving very good evidence that the change in the net Poynting flux direction of ELF hiss as determined by the measurement is indeed a real effect. It is therefore concluded that large electric antenna impedances are not affecting the correlation measurements of ELF hiss.

As discussed in the previous section, the proportionality factor between $\langle E_y B_z \rangle$ and $\langle S_x \rangle$ is highly anisotropic at only two azimuthal orientations. Since ELF hiss has been continuously observed for time periods comparable to one-half the azimuthal rotation period, and since the large number of ELF hiss observations are expected to be statistically distributed over all azimuthal angular positions of the satellite, at least some, and most probably a very large number, of the

ELF hiss measurements were performed under conditions of a nearly isotropic (with respect to θ) proportionality factor, thus ensuring the validity of tne net Poynting flux determination. In addition, no systematic dependence of the correlation measurements on the deviations of the satellite from exact magnetic alignment has been observed for any of the ELF hiss cases studied. It is therefore concluded that errors in the magnetic alignment of the satellite did not affect the Poynting flux determinations for ELF hiss.

B. Interpretation of Results

The observations of downgoing ELF hiss over the entire range of altitude and invariant latitude under study is in agreement with previous evidence on the direction of propagation of ELF hiss. Kennel and Petschek [1966] suggested that the generation of VLF whistler-mode noise at high altitudes near the equatorial plane might account for the wave energy necessary to drive observed pitch-angle diffusion, resulting in particle precipitation into the ionosphere. Russell et al. [1969] have observed the frequent occurrence of steady ELF noise near the equator at all local times for L values less than 6 and at magnetic latitudes around 45° above L = 6 in the sunward hemisphere. In addition, Gurnett and Burns [1968] explained the sharp lower cutoff frequency of ELF hiss in the ionosphere in terms of the reflection of downward-propagating waves.

The observations of upgoing ELF hiss can be explained in terms of a propagation effect in which downgoing waves may propagate across the plasmapause to lower latitudes and be subsequently refracted upwards and trapped within the plasmasphere. This explanation is able to account for (1) the high-latitude cutoff of upgoing ELF hiss, (2) the decrease, during local night, of the minimum altitude at which upgoing ELF hiss is observed, and (3) the observation of upgoing ELF hiss with a low-frequency cutoff (see Figure 4).

In order to examine this propagation effect, consider a wave propagating down the geomagnetic field in the low-density region on the high-latitude side of the plasmapause boundary. The refractive index surface for this wave is shown in Figure 5(c). Also shown in Figure 5 is a plot of the refractive index for perpendicular propagation $n_{\pi/2}$ versus altitude in the plasmasphere for Injun 5 altitudes (Figure 5(a)) and a plot of the electron density N_e versus latitude at the plasmapause (Figure 7(b)). If the downgoing wave is not propagating exactly parallel ($\theta = 0$) to the geomagnetic field, then it can propagate across field lines to lower latitudes, thereby crossing the plasmapause boundary and entering a region of higher density. The density increase at the plasmapause may be as much as a factor of 5 to 10. By Snell's law, $n_{\parallel}$ will remain nearly constant across the horizontal gradient as the wave propagates into the higher density region. However, $n_\perp$ will increase with increasing electron density, thereby increasing the wave normal angle θ. Since θ is still less than $\pi/2$, the wave will continue to propagate downward. If, however, the wave is above the altitude at which $n_{\pi/2}$ in the plasmasphere is a minimum, $n_{\parallel}$ will decrease as the wave propagates downward, causing θ to finally become equal to $\pi/2$. At this point, $n_{\parallel}$ can no longer decrease and the wave will refract upwards ($\theta > \pi/2$). On the other hand, if the wave crosses the plasmapause boundary at an altitude below which a minimum in the refractive index for perpendicular propagation occurs, then the wave will be able to propagate into the lower ionosphere.

In order to investigate the behavior of the refractive index for perpendicular propagation $n_{\pi/2}$ as a function of altitude, $n_{\pi/2}$ was calculated in a computer program using several different ionospheric models computed by Colin and Dufour [1968] for solar minimum conditions. These models provide a suitable indication of the behavior of $n_{\pi/2}$ as functions of both altitude and local time. For daytime ionospheric models at solar minimum, the altitude at which a minimum in $n_{\pi/2}$ occurs ranges from approximately 1500 km to above 3000 km. For nighttime models, however, this altitude can decrease by a factor of two to three, to well below 1000 km. Thus, the propagation model described above can account for the fact that ELF hiss having an upward-directed net Poynting flux is observed below 1500 km only during local night. In addition, the ionospheric model programs indicated that there was no substantial dependence of the minimum $n_{\pi/2}$ altitude upon frequency over the frequency range of ELF hiss. This is in agreement with the observations which show that the change in the net Poynting flux direction occurs at very nearly the same time at all frequencies (see Figure 4).

The propagation model presented above is also able to explain the observation of an upward-directed net Poynting flux at the lower frequency cutoff of ELF hiss. Consider again a wave propagating down the geomagnetic field just outside the plasmapause boundary. The two-ion cutoff frequency in this region will decrease with increasing altitude. At some given altitude h^*, only waves with frequencies greater than or equal to the local two-ion cutoff frequency f^* may be observed; all waves with frequencies less than f^* will have been reflected, outside the plasmasphere, at altitudes greater than h^*. The waves with frequencies greater than f^* which are able to propagate to altitudes below h^* may cross the plasmapause boundary and be refracted upwards, as discussed above. If the satellite is at or near the altitude h^* within the plasmasphere, these upgoing waves will be observed at the satellite. However, upgoing waves at frequencies less than f* will not be observed since they are not able to enter the plasmasphere below the satellite. Thus, a lower frequency cutoff of waves having an upward-directed net Poynting flux will be observed. Referring to Figure 4, it is seen that the observed cutoff frequency does not change appreciably as the plasmapause is crossed, in support of the conclusion that the cutoff frequency observed inside the plasmasphere in this case is actually near the two-ion cutoff frequency for downgoing waves outside the plasmasphere at the same altitude, rather than near the local two-ion cutoff frequency at the satellite as discussed by Gurnett and Burns [1968]. The observation of a cutoff frequency different from the local two-ion cutoff frequency can also explain the occasional observation, by several investigators, of a cutoff frequency above the local proton gyrofrequency (in a plasma, the local two-ion cutoff frequency is always less than the proton gyrofrequency). In Figure 4, for example, the local proton gyrofrequency increases from 255 Hz at 1412 UT to 305 Hz at 1418 UT, whereas the observed lower cutoff frequency of the ELF hiss band decreases from about 260 Hz to about 200 Hz over this period. The above observations provide further support for the explanation of the low-frequency cutoff of ELF hiss given by Gurnett and Burns [1968].

Other mechanisms have been considered as an explanation of the observations of upgoing ELF hiss in the plasmasphere. It has been suggested by Heyborne et al., [1969] that the observed cutoff of VLF signals beyond the plasmapause in the ionosphere might be due to a sharp increase in absorption in the lower ionosphere beyond the plasmapause. Such an absorption increase might provide for a relative absence of upgoing waves outside the plasmasphere while allowing downgoing waves to reflect and propagate upward within the plasmasphere. Such a mechanism, however, cannot account for the diurnal variation of the minimum altitude at which an upward-directed net Poynting flux is observed in the plasmasphere. It is therefore concluded that such reflections in the lower ionosphere can only contribute in small part, if at all, to the observed behavior of ELF hiss propagation. Similarly, a source of ELF hiss at low altitudes in the plasmasphere (in addition to sources at high altitudes) might successfully explain the observations of an upward-directed net Poynting flux in the plasmasphere, but it cannot explain the observation of a low-frequency cutoff in the upgoing waves.

III. VLF HISS

A. Results of Observations

The results of correlation measurements of VLF hiss from 40 Injun 5 revolutions support the preliminary results on VLF hiss presented by Mosier and Gurnett [1969]. In all 40 cases, VLF hiss was observed to have components propagating both up and down the geomagnetic field lines.

Several distinct forms of VLF hiss are observed in the Injun 5 data, all of which exhibit both upgoing and downgoing waves in the correlation measurement. Figure 6 illustrates the most commonly observed form of auroral-zone VLF hiss. This type of hiss has been discussed in detail by Gurnett [1966], who referred to it as impulsive hiss, and is characterized by spectral variations on a time scale of the order of a second and a lower cutoff frequency that tends initially to decrease with increasing latitude, reaching a minimum at about 70° INVL, and then tends to increase with increasing latitude [Gurnett, 1966]. This latitudinal frequency dependence is dramatically illustrated in Figure 7, which shows a transition between impulsive VLF hiss and a smoother form of hiss.

Figures 8 and 9 illustrate two types of V-shaped VLF hiss. This type of emission was first discussed by Gurnett [1966], who found that V-shaped hiss often occurred in association with intense fluxes of 10 keV precipitating electrons, using Injun 3 data. V-shaped hiss is characterized by narrow bands of emission which exhibit a smooth, steady variation of frequency with time. It may be symmetric in shape, as in Figure 8, from which the 'V-shaped' name is derived, or it may merely consist of segments of narrow emission bands, as in Figure 9. V-shaped hiss is often accompanied by a diffuse background of relatively weak VLF hiss which, like the V-shaped hiss, exhibits both upgoing <u>and</u> downgoing waves.

Illustrated in Figure 10 is a new type of VLF hiss which occurs commonly at sub-auroral latitudes and which is called mid-latitude hiss. Like auroral-zone hiss, it exhibits both upgoing and downgoing waves. However, whereas auroral-zone VLF hiss is seldom observed at latitudes <u>below</u> 65° INVL [Gurnett, 1966], mid-latitude hiss is not usually observed <u>above</u> 65° INVL. It is characterized by a narrow band of emission, of the order of 1 to 3 kHz in width, and exhibits a small latitudinal frequency dependence, the frequency decreasing with increasing latitude. Mid-latitude hiss is not generally of an impulsive nature like auroral-zone hiss, but rather quite smooth and steady in intensity. The lower frequency cutoff is usually quite sharp, while the upper frequency cutoff is more diffuse and ill-defined.

No dependence of the VLF hiss correlation results upon the deviation from spacecraft magnetic alignment or azimuthal orientation has been observed, and it is therefore concluded that the misorientation of the satellite is not affecting the Poynting flux determinations of VLF hiss.

B. Discussion of Results

Since VLF hiss is believed to occur almost entirely above the local LHR frequency [Jørgensen, 1968], it may not, in general, be possible to draw any definite conclusions concerning the direction of the net Poynting flux of VLF hiss. However, one can conclude from the observations of downgoing waves that at least part of the VLF hiss must be generated at altitudes above the satellite, since (1) upgoing waves cannot be reflected about the geomagnetic field line and (2) waves from the opposite hemisphere with frequencies greater than the equatorial electron gyrofrequency cannot propagate past the equator. The simultaneous observations of upgoing VLF hiss are probably due at least in part to the reflection of downgoing waves near the altitude at which the wave frequency is equal to the local LHR frequency, but there may also be additional emission of VLF hiss below the satellite. Although the present Poynting flux measurements of VLF hiss are consistent with emission mechanisms proposed by other investigators in which hiss is generated by Cerenkov radiation [see, for example, Jørgensen, 1968.], there is insufficient evidence from these measurements to draw any definite conclusions concerning the source mechanism.

IV. SAUCER-SHAPED EMISSIONS

The saucer-shaped emission was first reported by Mosier and Gurnett [1969], who explained the saucer envelope of the emissions in terms of a frequency-dependent limiting ray angle for propagation from a source at low altitude below the satellite. Since the initial data of Mosier and Gurnett [1969] were reported, six additional cases of saucer-shaped emissions have been studied; in each of these cases, the correlation measurement $\langle E_y B_z \rangle$ indicates only upgoing waves. These six cases represent all possible displacement directions for the satellite misalignment (refer to the discussion of misalignment errors in Paper 1) and it is expected that the data are distributed over different values of the azimuthal angular position of the satellite. As discussed in the introduction, there is a range of azimuthal orientations in which the proportionality factor between $\langle E_y B_z \rangle$ and $\langle S_x \rangle$ is nearly isotropic. Since it is highly unlikely that all measurements would have been made for azimuthal orientations having large anisotropies in the proportionality factor, one can conclude that the <u>absence</u> of downgoing waves in <u>all</u> of the measurements indicates that the net Poynting flux for the saucer-shaped emission is directed upwards.

V. SUMMARY

A new propagation phenomenon has been proposed for low altitudes in which downgoing ELF hiss may propagate across the plasmapause boundary to lower latitudes and become subsequently reflected and trapped within the plasmasphere. This propagation phenomenon is able to explain the following experimental observations:

(1) An upward-directed net Poynting flux of ELF hiss in certain regions of the plasmasphere.

(2) The diurnal variation of the minimum altitude at which an upward-directed net Poynting flux is observed.

(3) The low-frequency cutoff for upgoing ELF hiss.

(4) The low-frequency cutoffs of ELF hiss which occur above the local proton gyrofrequency.

Observations of VLF hiss indicate that at least some of the hiss is generated at altitudes above the Injun 5 satellite, although no definite conclusions can be made concerning the source mechanisms or the possibility of hiss generation below the satellite.

Observations of saucer-shaped emissions indicate that the net Poynting flux is directed upwards in all cases, in agreement with earlier results.

ACKNOWLEDGEMENTS

The author expresses his sincere appreciation to Professor D. A. Gurnett for his guidance, advice, and helpful suggestions throughout this study. The author also wishes to extend thanks to Professor J. A. Van Allen for his support and to Professor S. D. Shawhan for many helpful discussions. Special thanks are given to Dr. R. Sagalyn for providing data from the AFCRL electron density probe aboard Injun 5. The calibration and testing of the Injun 5 spacecraft required a considerable effort from Messrs. G. W. Pfeiffer, D. Odem, and R. R. Anderson, which is gratefully acknowledged. Part of this research was conducted while the author was a graduate trainee of the National Aeronautics and Space Administration. This research was submitted as a part of the author's Ph.D. dissertation at the University of Iowa.

This research was supported in part by the National Aeronautics and Space Administration under Contracts NAS5-10625, NAS1-8141, NAS1-8144(f), NAS1-8150(f), and NGR-16-001-043; and by the Office of Naval Research under Contract N00014-68-A-0196-0003.

REFERENCES

Carpenter, D. L., "Whistler studies of the plasmapause in the magnetosphere. 1. Temporal variations of the position of the knee and some evidence on plasma motions near the knee," J. Geophys. Res., 71, 693, 1966.

Carpenter, D. L., F. Walter, R. E. Barrington, and D. J. McEwen, "Alouette 1 and 2 observations of abrupt changes in whistler rate and of VLF noise variations at the plasmapause--a satellite-ground study," J. Geophys. Res., 73, 2929, 1968.

Colin, Lawrence, and Stuart W. Defour, "Charged particle temperatures and concentrations in the earth's exosphere," J. Geophys. Res., 73, 2967, 1968.

Gurnett, Donald A., "A satellite study of VLF hiss," J. Geophys. Res., 71, 5599, 1966.

Gurnett, Donald A., and Thomas B. Burns, "The low-frequency cutoff of ELF emissions," J. Geophys. Res., 73, 7437, 1968.

Gurnett, Donald A., G. William Pfeiffer, Roger R. Anderson, Stephen R. Mosier, and David P. Cauffman, "Initial observations of VLF electric and magnetic fields with the Injun 5 satellite," J. Geophys. Res., 74, 4631, 1969.

Heyborne, R. L., R. L. Smith, and R. A. Helliwell, "Latitudinal cutoff of VLF signals in the ionosphere," _J. Geophys. Res._, _74_, 2393, 1969.

Jørgensen, T. Stockflet, "Interpretation of auroral hiss measured on OGO 2 and at Byrd Station in terms of incoherent Cerenkov radiation," _J. Geophys. Res._, _73_, 1055, 1968.

Kennel, C. F., and H. E. Petschek, "Limit on stably trapped particle fluxes," _J. Geophys. Res._, _71_, 1, 1966.

Mosier, Stephen R., and Donald A. Gurnett, "VLF measurements of the Poynting flux along the geomagnetic field with the Injun 5 satellite," _J. Geophys. Res._, _74_, 5675, 1969.

Mosier, Stephen R., and Donald A. Gurnett, "The Theory of VLF Poynting flux measurements with the Injun 5 satellite," submitted to _J. Geophys. Res._, 1970.

Russell, Christopher, T., Robert E. Holzer, and Edward J. Smith, "OGO 3 observations of ELF noise in the magnetosphere. 1. Spatial extent and frequency of occurrence," _J. Geophys. Res._, _74_, 755, 1969.

Taylor, H. A., Jr., H. C. Brinton, D. L. Carpenter, F. M. Bonner, and R. L. Heyborne, "Ion depletion in the high-latitude exosphere; simultaneous OGO 2 observations of the light ion trough and the VLF cutoff," _J. Geophys. Res._, _74_, 3517, 1969.

FIGURE CAPTIONS

Figure 1. Top view of the Injun 5 satellite showing the orientation of the electric dipole and magnetic loop antenna.

Figure 2. Injun 5 orbit plots for times during which down-going ELF hiss was observed.

Figure 3. Injun 5 orbit plots for times during which upgoing ELF hiss was observed. No upgoing hiss was observed at altitudes greater than approximately 60° INVL.

Figure 4. Correlation measurement of ELF hiss for a plasma-pause crossing in which a transition from upgoing to downgoing waves occurred. The electron density from the AFCRL probe is also plotted and indicates that the transition occurs at the decrease in the electron density gradient.

Figure 5. Diagram showing reflection mechanism of ELF hiss in the plasmasphere.

Figure 6. Correlation measurement of impulsive auroral-zone VLF hiss, showing both downgoing and upgoing waves.

Figure 7. Correlation measurement of auroral-zone VLF hiss showing strong latitudinal dependence of lower cutoff frequency.

Figure 8. Correlation measurement of a symmetric V-shaped VLF hiss event showing both downgoing and upgoing waves.

Figure 9. Correlation measurement of V-shaped VLF hiss event consisting of segments of narrow emission bands, showing both downgoing and upgoing waves.

Figure 10. Correlation measurement of mid-latitude VLF hiss, showing both downgoing and upgoing waves. This type of hiss is observed at latitudes below about 65° INVL.

G68-1050-1

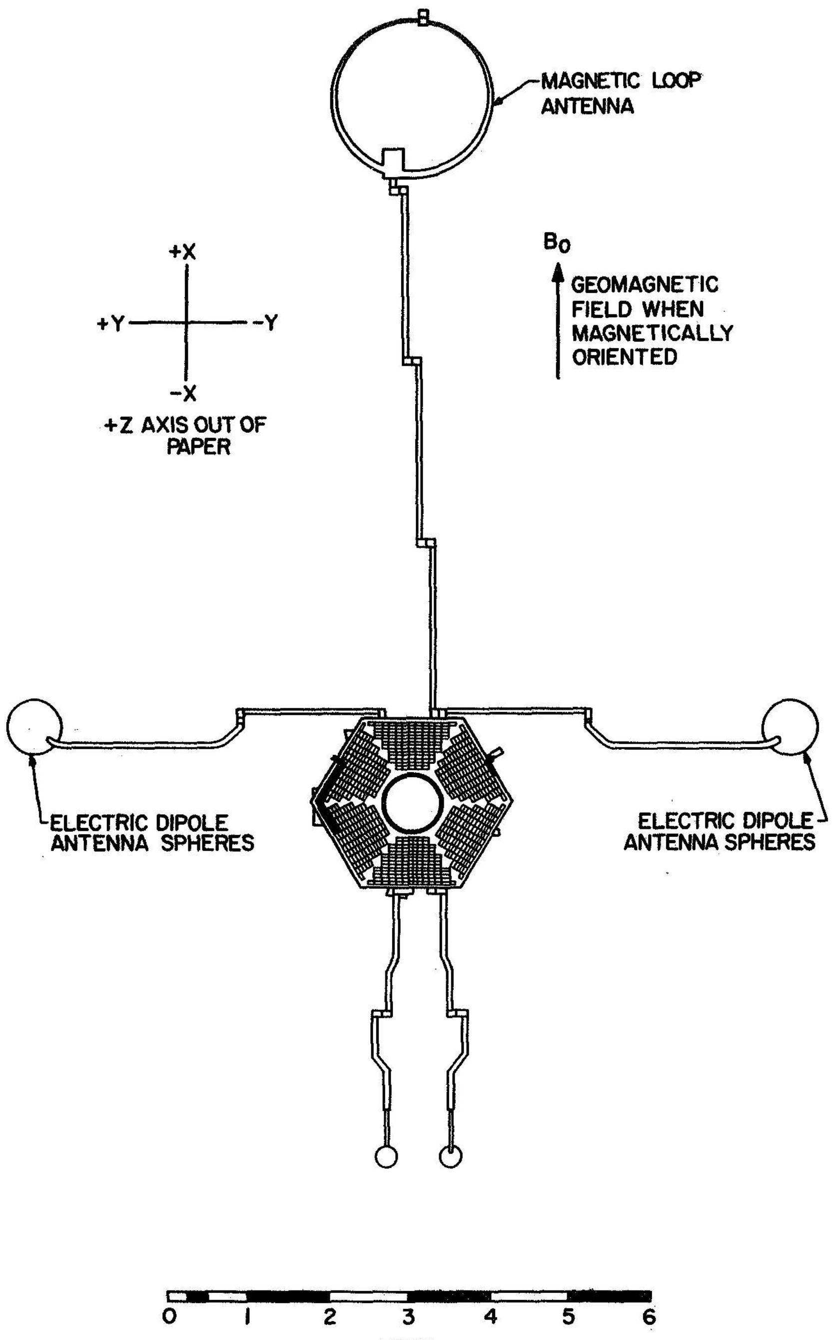

TOP VIEW
OF INJUN V

Figure 1

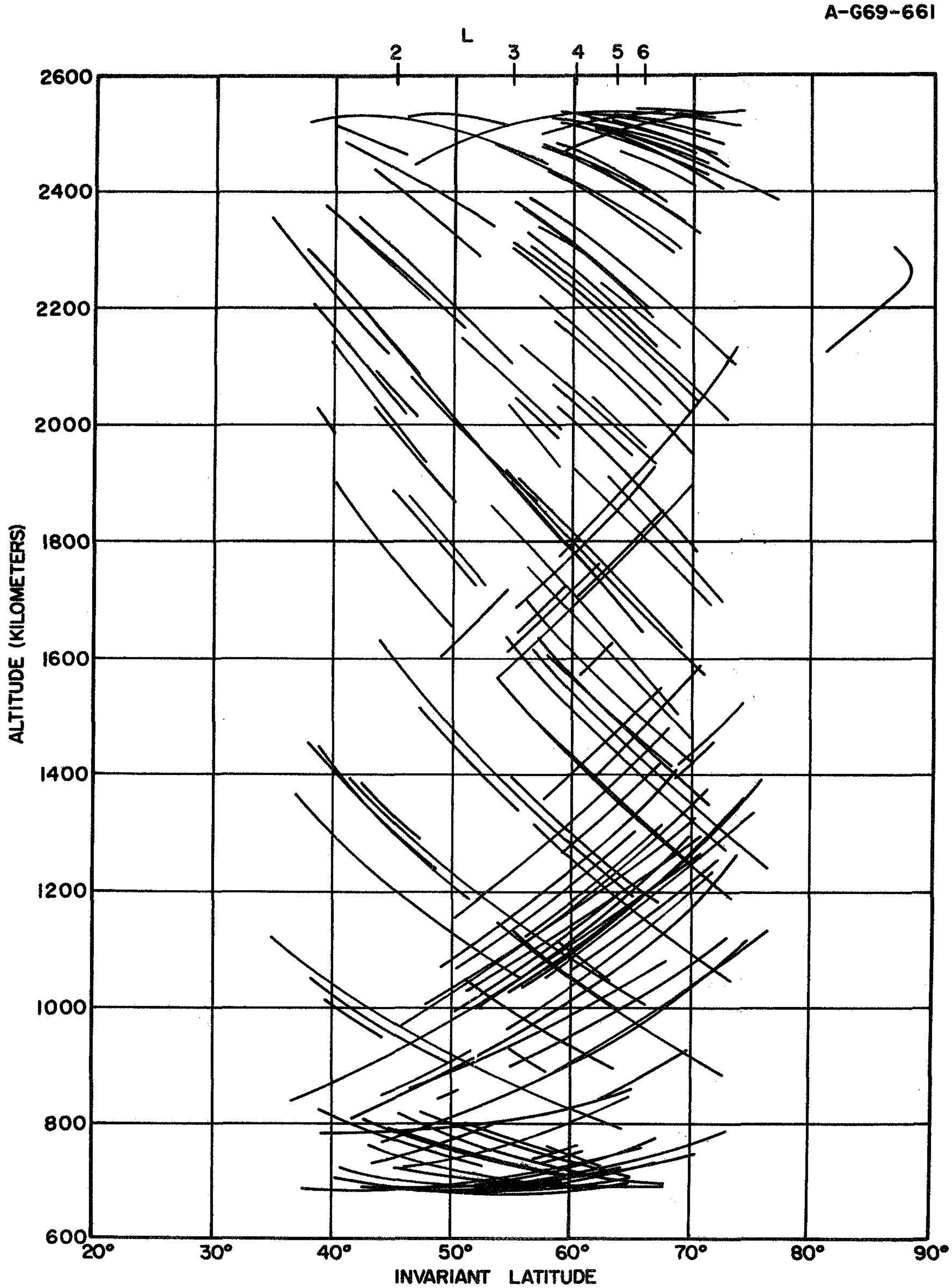
A-G69-661
L
2
3
4
5
6
2600
2400
2200
2000
1800
1600
1400
1200
1000
800
600
ALTITUDE (KILOMETERS)
20°
30°
40°
50°
60°
70°
80°
90°
INVARIANT LATITUDE

Figure 2

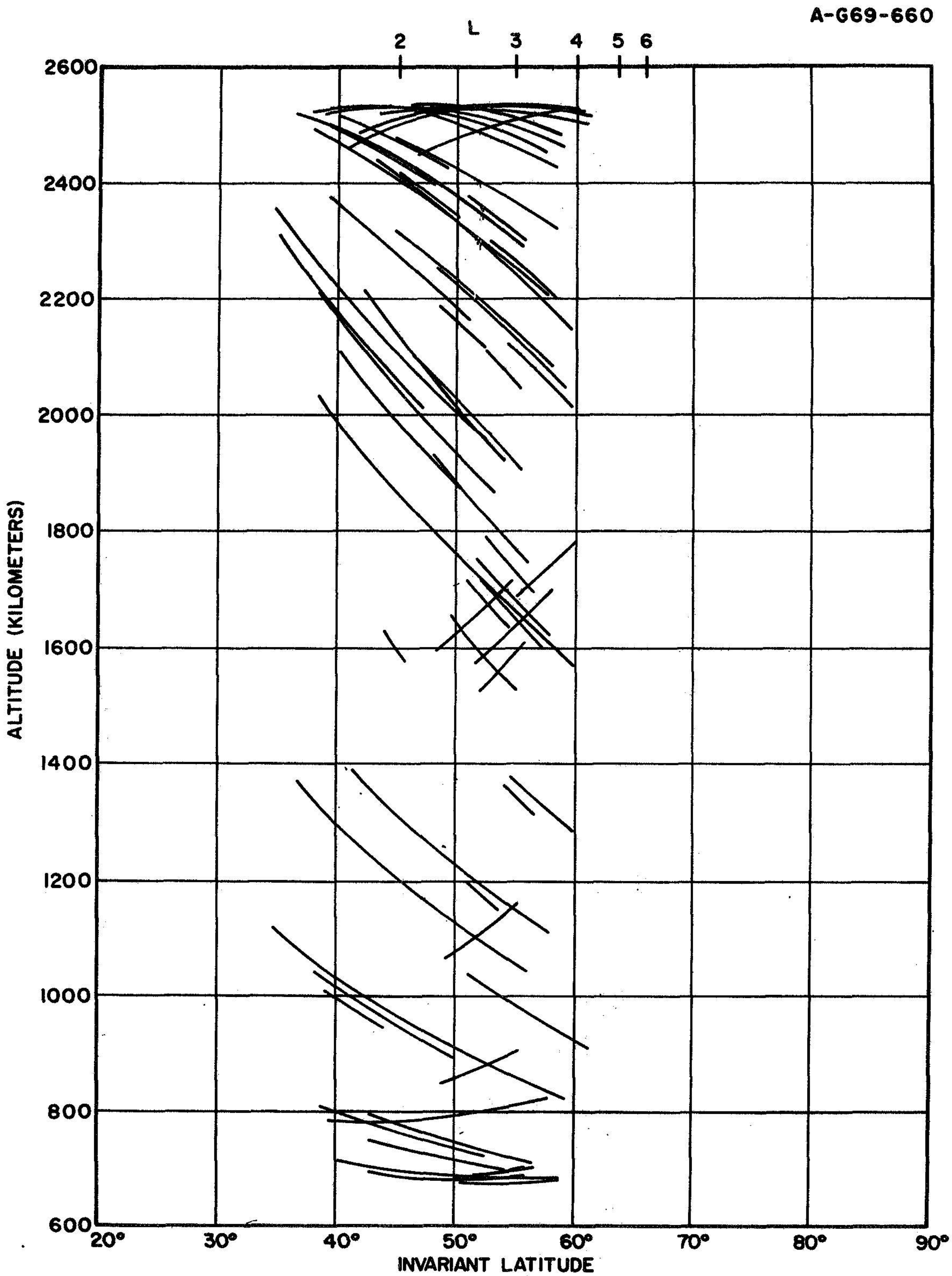
A-G69-660
L
2
3
4
5
6
2600
2400
2200
2000
1800
1600
1400
1200
1000
800
600
ALTITUDE (KILOMETERS)
20°
30°
40°
50°
60°
70°
80°
90°
INVARIANT LATITUDE

Figure 3

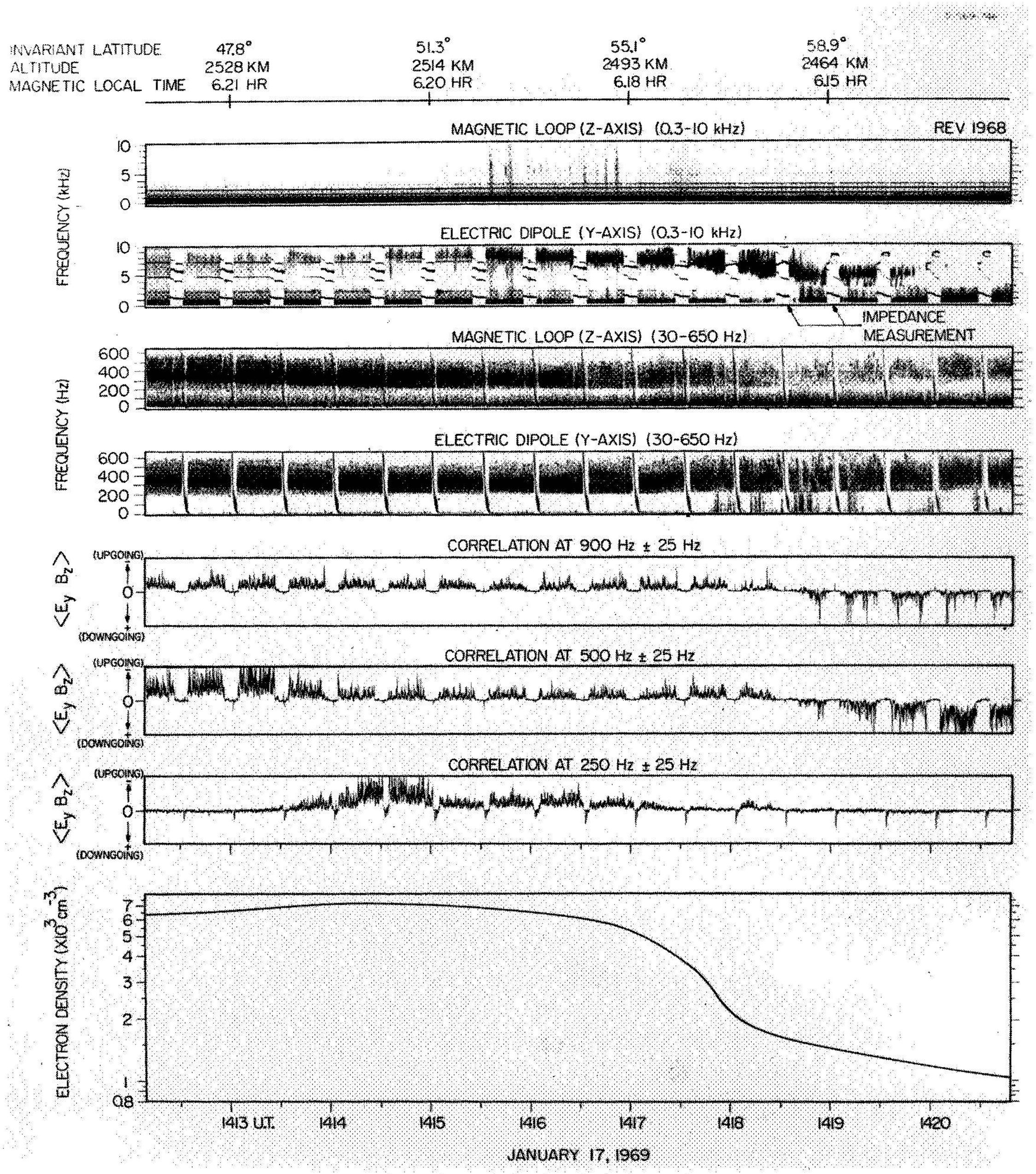

INVARIANT LATITUDE
ALTITUDE
MAGNETIC LOCAL TIME
47.8°
2528 KM
6.21 HR
51.3°
2514 KM
6.20 HR
55.1°
2493 KM
6.18 HR
58.9°
2464 KM
6.15 HR
MAGNETIC LOOP (Z-AXIS) (0.3-10 kHz)
REV 1968
ELECTRIC DIPOLE (Y-AXIS) (0.3-10 kHz)
FREQUENCY (kHz)
IMPEDANCE
MEASUREMENT
MAGNETIC LOOP (Z-AXIS) (30-650 Hz)
ELECTRIC DIPOLE (Y-AXIS) (30-650 Hz)
FREQUENCY (Hz)
CORRELATION AT 900 Hz ± 25 Hz
CORRELATION AT 500 Hz ± 25 Hz
CORRELATION AT 250 Hz ± 25 Hz
(UPGOING)
(DOWNGOING)
⟨Ey Bz⟩
ELECTRON DENSITY (X10^3 cm^-3)
1413 U.T.
1414
1415
1416
1417
1418
1419
1420
JANUARY 17, 1969

Figure 4

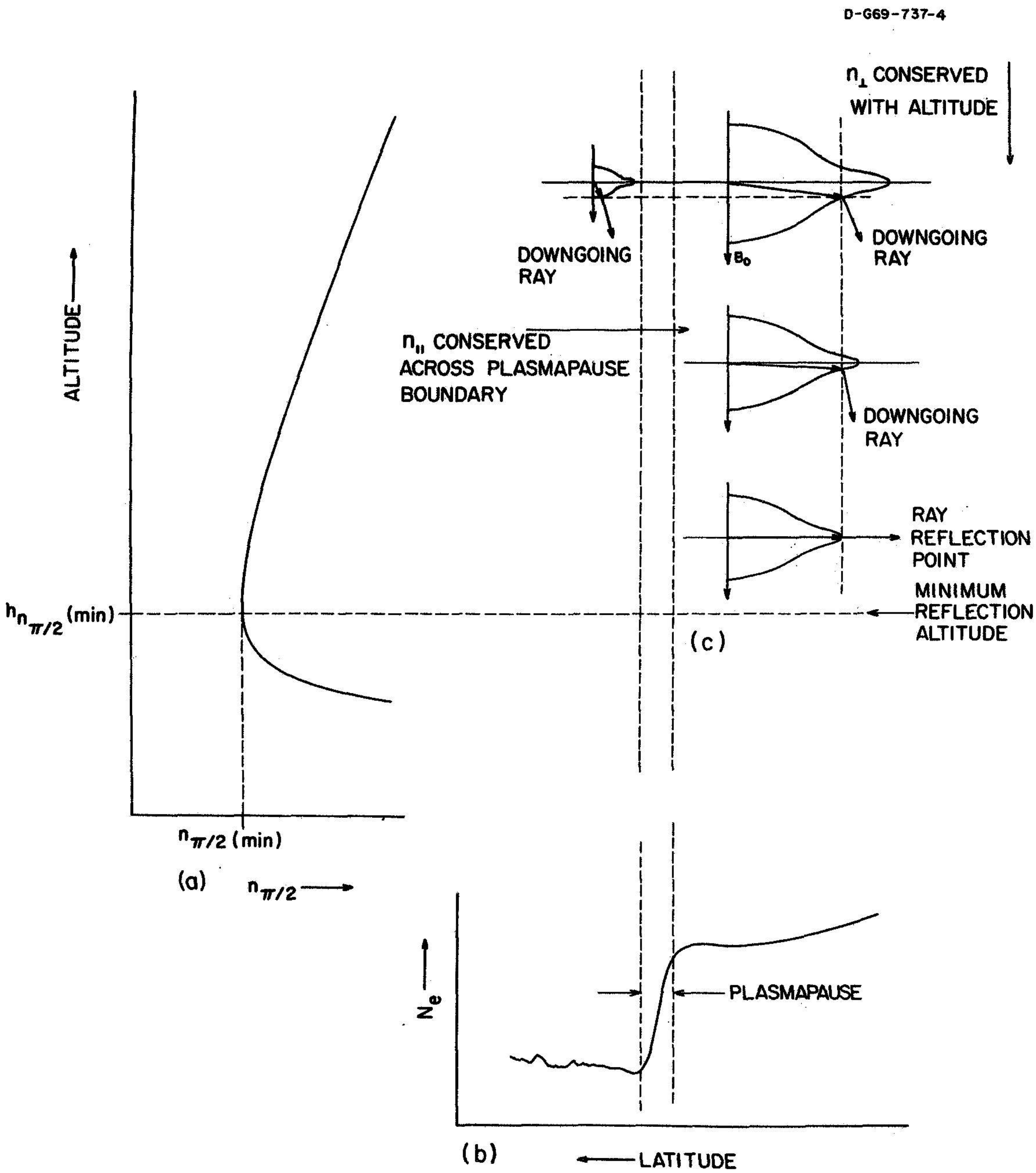
D-G69-737-4
$n_\perp$ CONSERVED
WITH ALTITUDE
DOWNGOING
RAY
B_0
DOWNGOING
RAY
$n_\parallel$ CONSERVED
ACROSS PLASMAPAUSE
BOUNDARY
DOWNGOING
RAY
RAY
REFLECTION
POINT
MINIMUM
REFLECTION
ALTITUDE
(c)
ALTITUDE
$h_{n_{\pi/2}}$(min)
$n_{\pi/2}$(min)
(a)
$n_{\pi/2}$
N_e
PLASMAPAUSE
(b)
LATITUDE

Figure 5

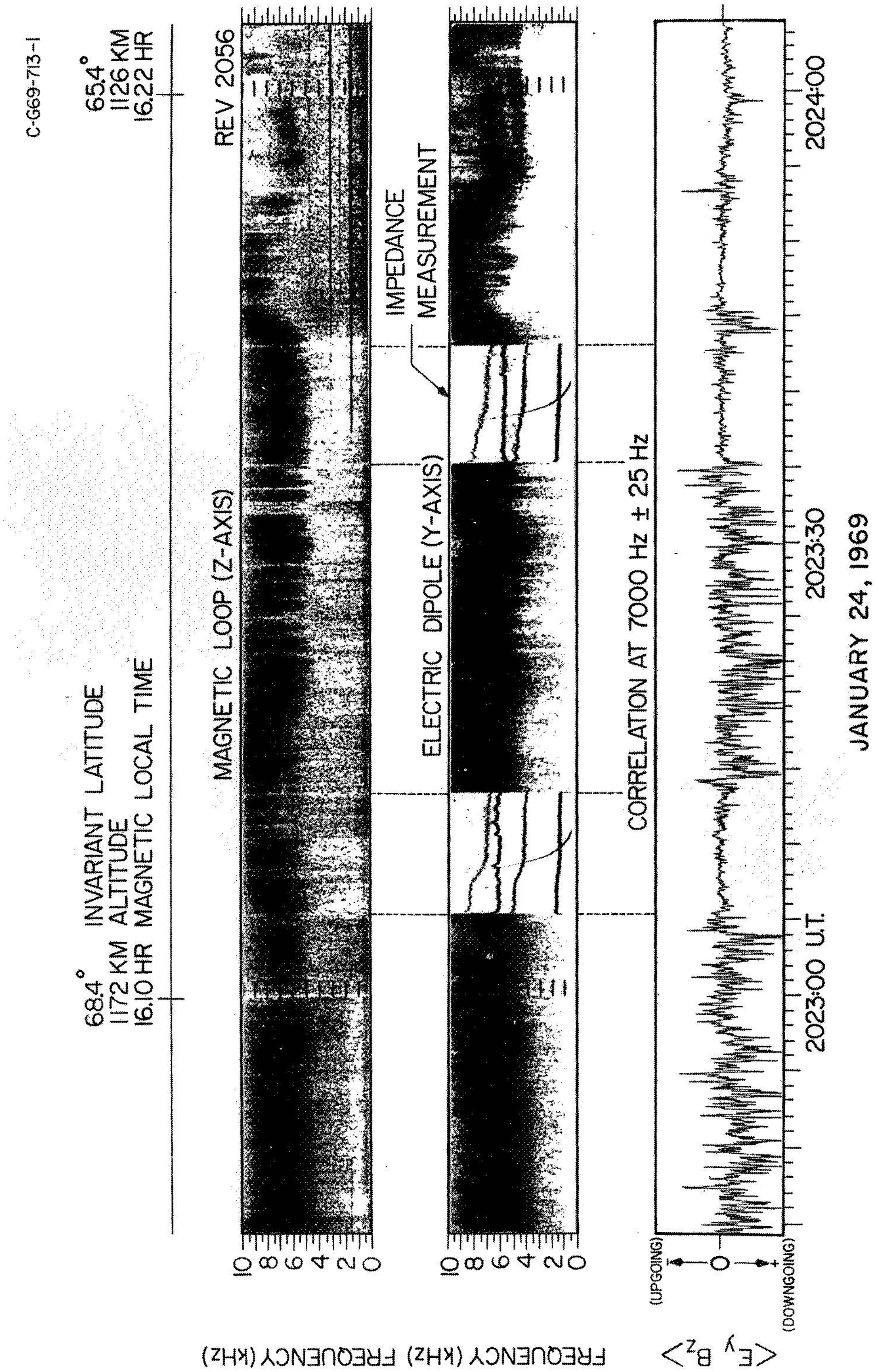
C-G69-713-1
68.4° INVARIANT LATITUDE
1172 KM ALTITUDE
16.10 HR MAGNETIC LOCAL TIME
65.4°
1126 KM
16.22 HR
REV 2056
MAGNETIC LOOP (Z-AXIS)
IMPEDANCE MEASUREMENT
ELECTRIC DIPOLE (Y-AXIS)
CORRELATION AT 7000 Hz ± 25 Hz
FREQUENCY (kHz)
FREQUENCY (kHz)
10 8 6 4 2 0
10 8 6 4 2 0
$\langle E_y B_z \rangle$
(UPGOING)
0
(DOWNGOING)
2023:00 U.T.
2023:30
2024:00
JANUARY 24, 1969

Figure 6

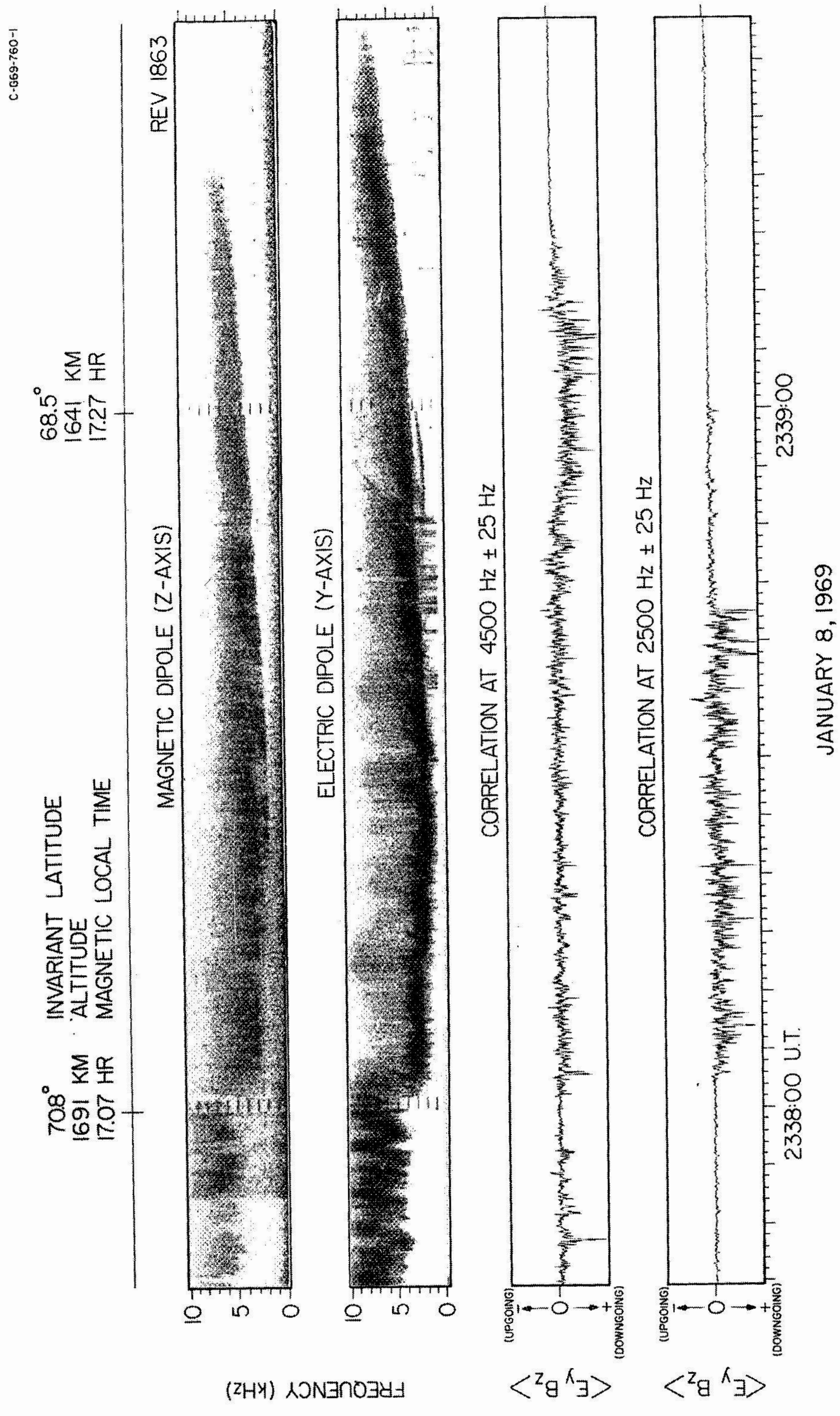

C-G69-760-1
REV 1863
68.5°
1641 KM
17.27 HR
70.8°
1691 KM
17.07 HR
INVARIANT LATITUDE
ALTITUDE
MAGNETIC LOCAL TIME
MAGNETIC DIPOLE (Z-AXIS)
ELECTRIC DIPOLE (Y-AXIS)
CORRELATION AT 4500 Hz ± 25 Hz
CORRELATION AT 2500 Hz ± 25 Hz
FREQUENCY (kHz)
10
5
0
(UPGOING)
(DOWNGOING)
2338:00 U.T.
2339:00
JANUARY 8, 1969

Figure 7

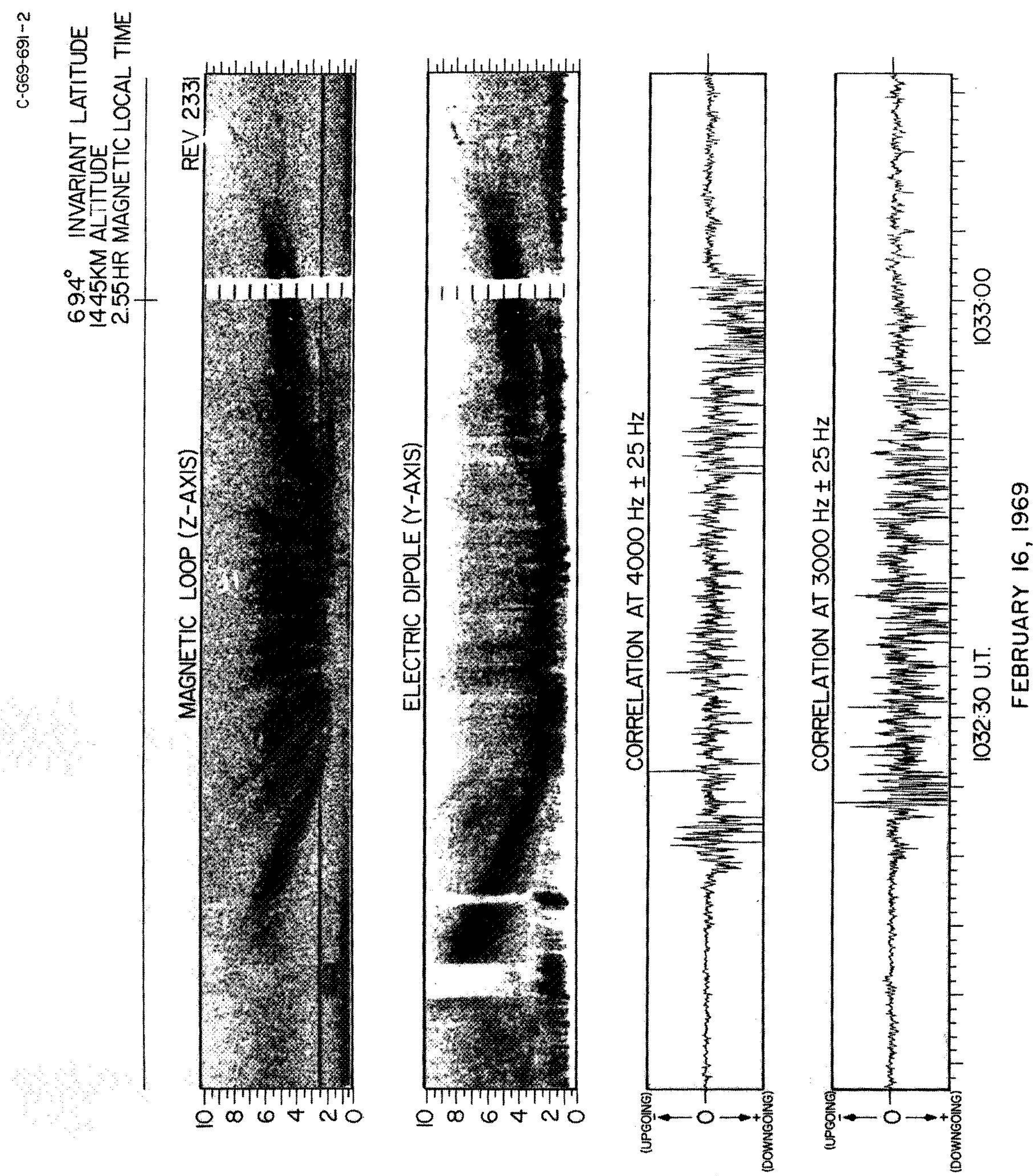

C-G69-691-2
69.4° INVARIANT LATITUDE
1445KM ALTITUDE
2.55HR MAGNETIC LOCAL TIME
REV 2331
MAGNETIC LOOP (Z-AXIS)
FREQUENCY (KHz)
10
8
6
4
2
0
ELECTRIC DIPOLE (Y-AXIS)
FREQUENCY (KHz)
10
8
6
4
2
0
CORRELATION AT 4000 Hz ± 25 Hz
$\langle E_y B_z \rangle$
(UPGOING)
0
(DOWNGOING)
CORRELATION AT 3000 Hz ± 25 Hz
$\langle E_y B_z \rangle$
(UPGOING)
0
(DOWNGOING)
1033:00
1032:30 U.T.
FEBRUARY 16, 1969

Figure 8

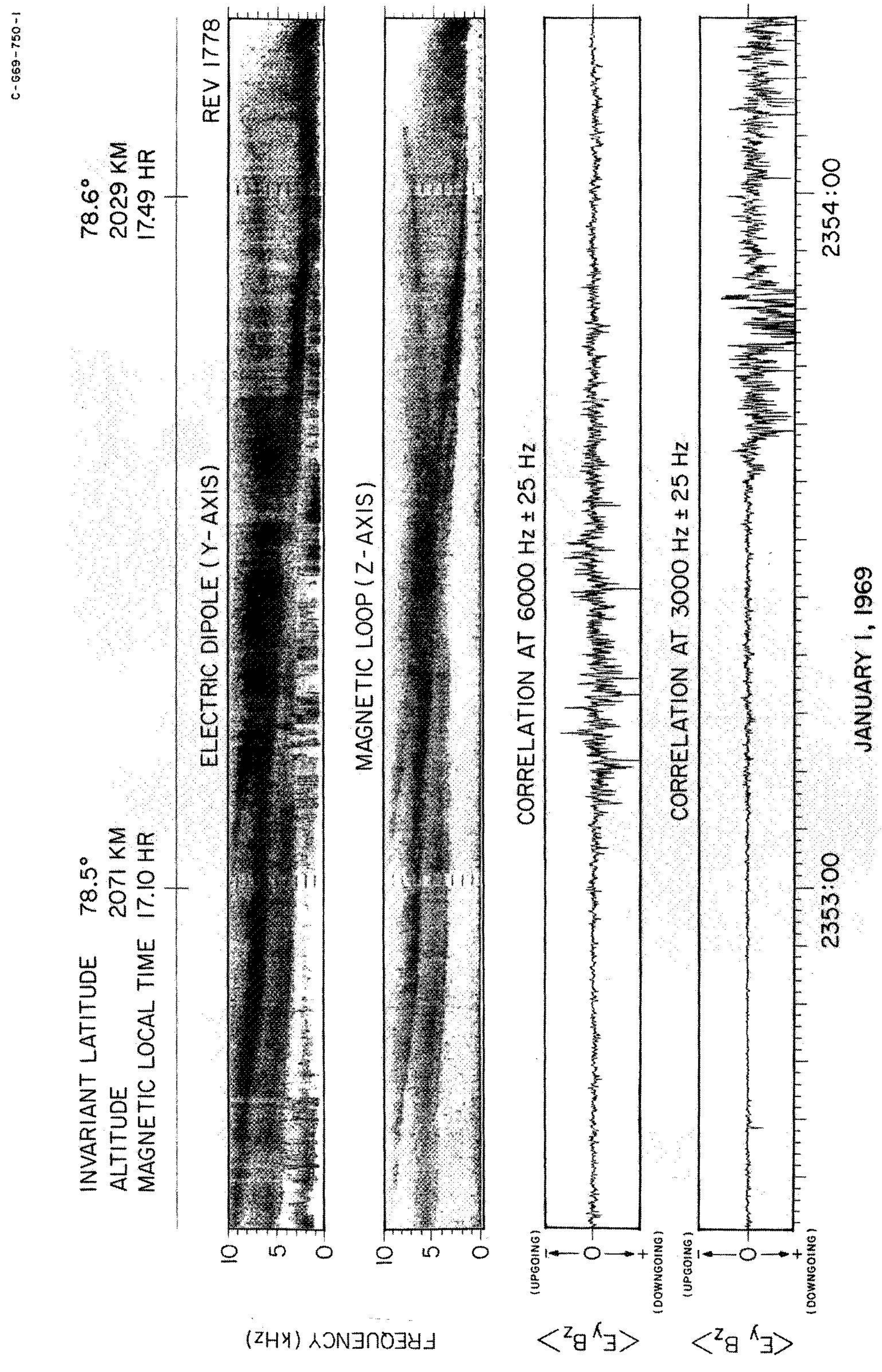
C-G69-750-1
INVARIANT LATITUDE 78.5°
ALTITUDE 2071 KM
MAGNETIC LOCAL TIME 17.10 HR
78.6°
2029 KM
17.49 HR
REV 1778
ELECTRIC DIPOLE (Y-AXIS)
MAGNETIC LOOP (Z-AXIS)
FREQUENCY (kHz)
10
5
0
CORRELATION AT 6000 Hz ± 25 Hz
CORRELATION AT 3000 Hz ± 25 Hz
$\langle E_y B_z \rangle$
(UPGOING)
(DOWNGOING)
2353:00
2354:00
JANUARY 1, 1969

Figure 9

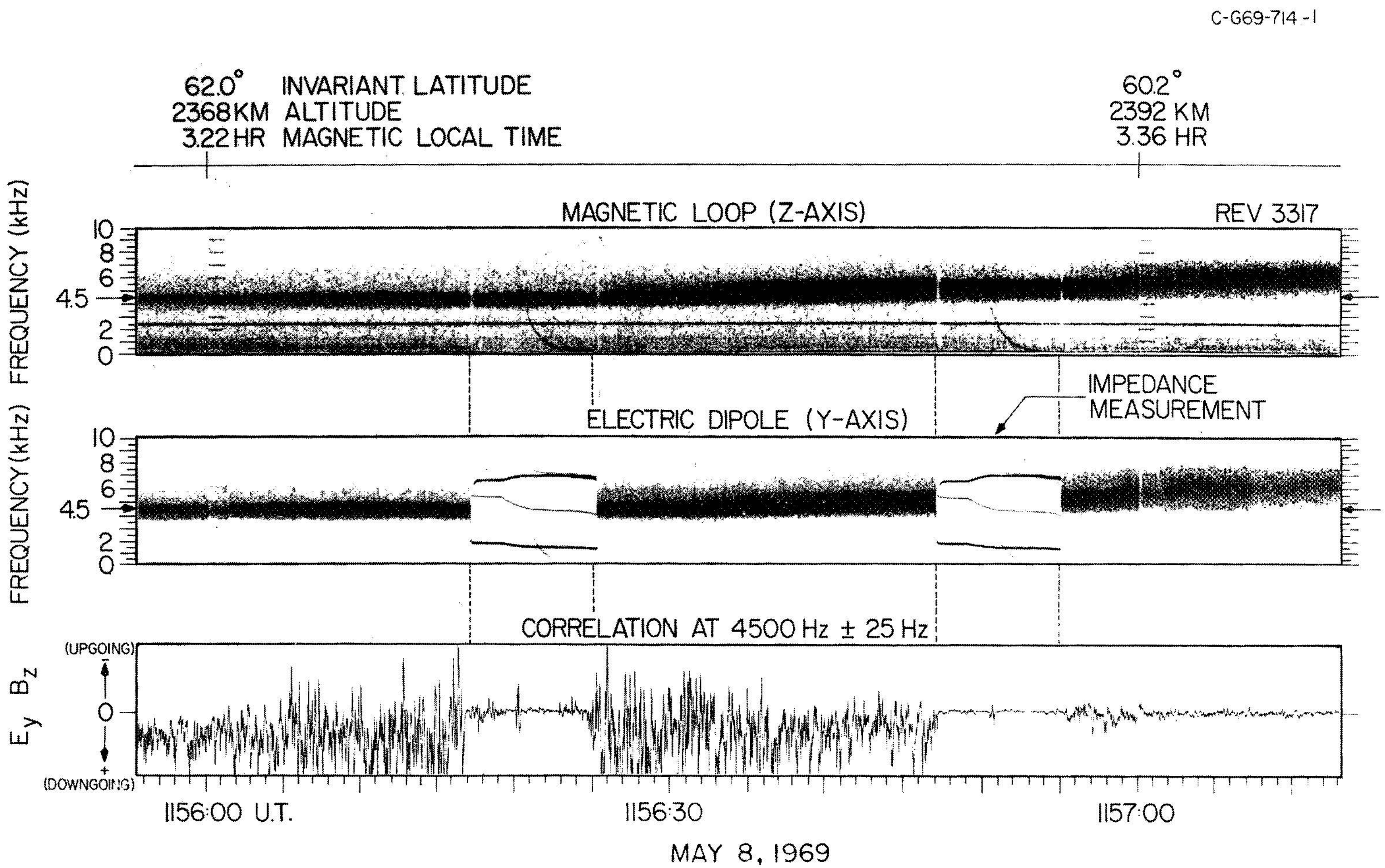
C-G69-714 -1
62.0° INVARIANT LATITUDE
2368 KM ALTITUDE
3.22 HR MAGNETIC LOCAL TIME
60.2°
2392 KM
3.36 HR
MAGNETIC LOOP (Z-AXIS)
REV 3317
FREQUENCY (kHz)
10
8
6
4.5
2
0
IMPEDANCE
MEASUREMENT
ELECTRIC DIPOLE (Y-AXIS)
FREQUENCY (kHz)
CORRELATION AT 4500 Hz ± 25 Hz
(UPGOING)
Ey Bz
0
(DOWNGOING)
1156:00 U.T.
1156:30
1157:00
MAY 8, 1969

Figure 10